Forests **2015**, *6*, 3218-3236; doi:10.3390/f6093218

OPEN ACCESS

forests

ISSN 1999-4907

www.mdpi.com/journal/forests

Article

Accuracy of Kinematic Positioning Using Global Satellite Navigation Systems under Forest Canopies

Harri Kaartinen [1,*], Juha Hyyppä [1], Mikko Vastaranta [2], Antero Kukko [1,3], Anttoni Jaakkola [1], Xiaowei Yu [1], Jiri Pyörälä [1], Xinlian Liang [1], Jingbin Liu [1], Yungshen Wang [1], Risto Kaijaluoto [1], Timo Melkas [4], Markus Holopainen [2] and Hannu Hyyppä [3]

[1] Finnish Geospatial Research Institute FGI, Centre of Excellence in Laser Scanning Research, Geodeetinrinne 2, Masala FI-02430, Finland; E-Mails: juha.coelasr@gmail.com (J.H); antero.kukko@nls.fi (A.K.); anttoni.jaakkola@nls.fi (A.J.); xiaowei.yu@nls.fi (X.Y.); jiri.pyorala@nls.fi (J.P.); xinlian.liang@nls.fi (X.L.); jingbin.liu@nls.fi (J.L.); yunsheng.wang@nls.fi (Y.W.); risto.kaijaluoto@nls.fi (R.K.)

[2] Department of Forest Sciences, University of Helsinki, P.O. Box 27, Helsinki FI-00014, Finland; E-Mails: mikko.vastaranta@helsinki.fi (M.V.); markus.holopainen@helsinki.fi (M.H.)

[3] Research Institute of Modelling and Measuring for the Built Environment, Aalto University, P.O. Box 15800, Aalto FI-00076, Finland; E-Mail: hannu.hyyppa@aalto.fi

[4] Metsäteho Oy, Vernissakatu 4, Vantaa FI-01300, Finland; E-Mail: timo.melkas@metsateho.fi

***** Author to whom correspondence should be addressed; E-Mail: harri.kaartinen@nls.fi; Tel.: +358-401-920-836.

Academic Editor: Eric J. Jokela

Received: 23 July 2015 / Accepted: 9 September 2015 / Published: 16 September 2015

Abstract: A harvester enables detailed roundwood data to be collected during harvesting operations by means of the measurement apparatus integrated into its felling head. These data can be used to improve the efficiency of wood procurement and also replace some of the field measurements, and thus provide both less costly and more detailed ground truth for remote sensing based forest inventories. However, the positional accuracy of harvester-collected tree data is not sufficient currently to match the accuracy per individual trees achieved with remote sensing data. The aim in the present study was to test the accuracy of various instruments utilizing global satellite navigation systems (GNSS) in motion under forest canopies of varying densities to enable us to get an understanding of the current state-of-the-art in GNSS-based positioning under forest canopies. Tests were conducted using several different combinations of GNSS and inertial measurement unit (IMU) mounted

on an all-terrain vehicle (ATV) "simulating" a moving harvester. The positions of 224 trees along the driving route were measured using a total-station and real-time kinematic GPS. These trees were used as reference items. The position of the ATV was obtained using GNSS and IMU with an accuracy of 0.7 m (root mean squared error (RMSE) for 2D positions). For the single-frequency GNSS receivers, the RMSE of real-time 2D GNSS positions was 4.2–9.3 m. Based on these results, it seems that the accuracy of novel single-frequency GNSS devices is not so dependent on forest conditions, whereas the performance of the tested geodetic dual-frequency receiver is very sensitive to the visibility of the satellites. When post-processing can be applied, especially when combined with IMU data, the improvement in the accuracy of the dual-frequency receiver was significant.

Keywords: GNSS; accuracy; forest mapping; forest inventory; positioning; harvester; forest technology

1. Introduction

Airborne laser scanning (ALS) is increasingly being used in forest mapping [1–3]. In certain types of mature stands, even individual trees can be inventoried using ALS data [4–6]. This kind of individual-tree-level inventory is usually based on the detection of trees from an ALS point cloud. The estimation of the tree variables is based on ALS-derived point cloud metrics and ground-truth data corresponding to the same trees [7–9], thus creating a geodatabase for accurate tree inventory.

In Finland, 96% of annual timber felling in standing sales on privately-owned forestland is done using harvesters [10]. As part of the harvesting process, a harvester collects detailed data on the logged trees, such as length of the utilizable stem part and stem diameter at intervals of 10 cm; and the length, top diameter, and volume of each log [11]. The majority of harvesters are equipped with a global navigation satellite system (GNSS), in addition to having onboard geographic information system (GIS) software. Currently, the location of a harvester under the forest canopy is recorded with an accuracy of about 3 m [12], but the location of the harvester head, *i.e.*, the location of the processed tree, is not recorded. However, only the roundwood trade and haulage are based on these harvester measurements.

Information collected by means of the harvester head could partly replace the field measurements needed for calibrating remotely-sensed inventory data, and thereby provide both less costly and more detailed reference data required in various forest inventory and mapping applications. Holopainen *et al.* [13] proposed that after harvesting a few trees, local inventory data can be updated in real time. However, the positional accuracy of the current harvester-based tree data is not sufficient to match the trees detected by ALS and therefore harvester head positioning requires technical improvements. There are technical solutions that could be used for positioning the harvester head relative to the harvester, but so far there have not been enough incentives for machine manufacturers to add this new functionality to new machines. If the harvester is also equipped with a MLS (Mobile Laser Scanning) system, then trees possessing the desired characteristics could be selected using the stem curve information available from the MLS data. Moreover, the direct georeferencing solution of GNSS/IMU sensors could be used in the positioning of such a harvester.

Thus, improved performance in forest inventory is expected to be achieved if the position of the harvester head is known so that the harvested trees and the ALS data can be linked. Some studies have been conducted explaining the usability of the approach. Peuhkurinen *et al.* [6] conducted the first tests where ALS data were used in making pre-harvest measurements. An inventory based on individual tree crowns (ITC) was carried out in two mature conifer stands (density ~465 stems per hectare) prior to logging. The major problem in ITC is deemed to be tree detection (e.g., [14,15]), but on a managed forest site tested in the study the number of harvestable trees was underestimated by less than 3%. In general, the ITC approach is at its best in single-layered mature stands. Holmgren *et al.* [16] showed that if the harvester measurements are used as reference data for ALS-based tree-level inventories, highly accurate estimates can be obtained. Their imputation accuracies (root mean squared error percentage RMSE-%) for stem volume, mean tree height, mean stem diameter, and stem density were 11%, 8%, 12%, and 19%, respectively. These validations were executed using aggregated plots, which suggests that stand-level estimates would be even more accurate. Since tree positions were missing from operational harvester data, Holmgren *et al.* [16] used manual measurements to match the logged trees with the ALS data. Holmgren *et al.* [16], like Holopainen *et al.* [13], also stated that a future operational system could continuously receive stem data sent from the operating harvester and these data could be used to continuously update an ALS-based reference database, and thereby enable improved prediction of stem attributes for stands not yet harvested. Melkas *et al.* [17] studied forest resource data updating using a harvester's species-specific timber volume data. In that study, the pre-thinning ALS-derived accuracies (RMSE-%) were 21.6% and 21.7% for an area-based ALS inventory (see [18]) and ITC-based inventory, respectively (validated pre-felling by means of field-measured plots). Following the thinning operation, the timber volume data were updated based on the harvester data, and the corresponding RMSE-% values were 29.4% and 31.6%. However, the absolute RMSE values remained at the pre-felling level. Melkas *et al.* [17] concluded that harvester data have potential for updating stand-level data. If sophisticated databases showing the locations and species of individual trees are available, tree-level harvest scheduling can be optimized; e.g., by using a species-mingling index as suggested by Bettinger and Tang [19].

The aim in this study was to test the accuracy of various instruments utilizing GNSS mounted on machinery in motion under forest canopies of varying densities to enable us to understand the current state-of-the-art in GNSS-based positioning under forest canopies. The tested GNSS devices include a low-cost, consumer handheld navigator, two single-frequency receivers with external mini-antennas, and a geodetic dual-frequency receiver with an external antenna. Both real-time positioning and post-processed positioning with and without inertial measurement unit (IMU) data were analyzed to find out what kind of equipment could be added to the harvesters to achieve the required positioning performance for reliable tree matching. In the future, the stem data collected by means of harvesters could be used for enhancing pre-harvest inventory data to predict logging yields from forest stands. There is a high operational requirement for these kind of high-resolution forest data. Modern wood flow optimization tools could be used more efficiently and provide savings through precision forestry.

2. Positioning in the Forest

2.1. Global Navigation Satellite Systems (GNSS)

Satellite-based positioning includes deriving the location of a user's receiver based on radio frequency signals transmitted by satellite systems. Current fully-operational GNSS applications include the US Navstar GPS (Global Positioning System) and the Russian GLONASS (GLObalnaja NAvigatsionnaja Sputnikovaja Sistema). Satellite-based positioning is based on accurate time determination: the time difference between the transmitted and the received radio signal denotes the signal travel time, which reveals the distance between the satellite and the user's antenna. Utilizing these measurements of the distance between the user antenna and a minimum of four different satellites, the receiver can obtain three-dimensional receiver coordinates in a global reference frame and the time difference between the receiver and the satellite's clocks.

Satellite-based positioning is undergoing a period of rapid change. There is a need to reform the GPS and GLONASS systems due to the increasing number of applications, more demanding requirements from users, and the need to mitigate interference and disturbances to the radio signals used by these systems. Both of these systems are being modernized to better serve the challenging present-day applications in obstructed signal conditions. These modernizations include an increasing the number of transmission frequencies and changes to signal components. In addition, the European Galileo and the Chinese BeiDou systems are under development. There is a determined intention to design the future, modernized systems to be resistant to interference, as well as to be more accurate and available over a wider range of conditions. Also, the use of multiple systems for positioning increases the accuracy and reliability of positioning even further [20].

2.1.1. GPS

The GPS is maintained and financed by the US Department of Defense and currently consists of 31 operational satellites orbiting at an altitude of about 20,200 km [21]. These satellites transmit signals primarily at two frequencies called L1 and L2. In the future, GPS satellites will also transmit a signal called L5. Two types of pseudorandom codes are modulated in GPS signal transmission onto the carrier signal: a civilian Coarse Acquisition (C/A) code is modulated to carrier L1 and this is used for coarse positioning, and Precise (P) code is modulated to carriers L1 and L2 for precision positioning. In addition, a navigation message is modulated to the signal containing information about the satellites' orbits, clocks, and health status. Generally, only the C/A code is utilized in civilian receivers for obtaining the satellite-to-user distances and then the user location. Because the true difference between the satellite's and receiver's clocks is not known, the measured distance is called pseudorange. The C/A code enables the code's pseudorange to be derived with an accuracy of about 3 m. When the phase of the carrier signal is used, the phase pseudorange can be determined with an accuracy of a millimeter, but then the number of full waves, the ambiguity, must be either resolved by using the code pseudorange or estimated. The loss of signal lock between a GPS satellite and the receiver is referred to as cycle slip, following which the ambiguity must be resolved. The use of a dual frequency receiver, utilizing both L1 and L2, allows the removal of the first-order effects of the ionosphere. [22] The more precise P code is mostly intended for military purposes. A GPS receiver obtains and processes signals simultaneously

from multiple satellites. When the satellite locations can be determined from the navigation message modulated to the signal, the different satellite-to-user distance measurements provide the means for calculating the user's receiver's position, velocity, and time [20].

2.1.2. GLONASS

Following the recent years' vigorous maintenance and reformation efforts, Russia's satellite navigation system GLONASS is again fully operational. GLONASS differs from GPS especially as regards the scheme used for signal transmissions; each GLONASS satellite has its own transmission frequency and they orbit at an altitude of about 19,000 km. Currently, GLONASS has 24 operational satellites. GLONASS, like GPS, was originally designed for military purposes, but nowadays its applications have spread to uses such as land and sea traffic, and gradually to other consumer products. GLONASS continues to undergo modernization, and in the future GLONASS will also use code division technology in its signal transmissions like GPS (*i.e.*, all of the satellites will transmit on the same carrier frequency). New signals and codes are also being added to GLONASS in order to enable improved accuracy and interoperability with other systems [20].

2.1.3. Emerging Systems: Galileo and BeiDou

The European satellite navigation system, Galileo, is intended for civilian use and it has been under development for almost a decade. Problems in financing, design, and interoperability (with, for example, the US GPS) have delayed the plans for and deployment of the new system. One of the foremost motives for developing Galileo has been the goal of making it independent from the military-operated systems. Dependency on the other systems is considered to adversely impact European security and to bring about too much insecurity for all of the applications and services currently depending on satellite-based navigation. Two test satellites have already been in orbital operation since 2005 and 2008, and in October 2011 two of the first in-orbit validation satellites were launched successfully to their planned orbits, and a year later two more were launched. The Galileo system will consist of a total of 30 satellites orbiting at an altitude of about 23,000 km [23]. Galileo is expected to be fully operational around 2018–2020, and Galileo satellites will be transmitting signals on the same frequencies as GPS, but modulated using different code techniques [20].

The Chinese satellite navigation system under development, *i.e.*, BeiDou (COMPASS) Navigation Satellite System, is somewhat similar in design to the US GPS. BeiDou will consist of 35 satellites, five of which will orbit in geostationary orbits. The geostationary part will transmit differential error corrections related to GNSS signals. BeiDou is estimated to be operational in 2020 at the latest [20].

2.2. Positioning Accuracy and Augmentation Systems

The accuracy achievable using GNSS ranges from a few millimeters to tens of meters depending on the operating environment and receiver technology used (e.g., single- or dual-frequency use, code- or carrier-phase measurements, and static or kinematic receivers). Better positioning accuracy can be achieved using more complicated and thus more expensive technology. Millimeter accuracy can only be achieved in good, unobstructed signal conditions, such as those in open, outdoor areas, utilizing

differential GNSS (DGNSS). The basic concept of DGNSS is the use of a minimum of two receivers, one at a known location and one at an unknown position, which can see common GNSS satellites. By fixing the location of one of the receivers, the other location can be found either by computing corrections to the position of the unknown receiver or by computing corrections to the pseudoranges. Satellite signals are generally noisy, especially in environments where signals are attenuated and reflected, which is also called multi-pathing, due to obstacles in the proximity, such as buildings or trees.

Augmentation of GNSS means improving the navigation system's performance, such as accuracy, reliability, and availability, through the integration of external data into the positioning computation. Some systems transmit additional data on sources of error (such as clock drift, ephemeris, or ionospheric delay), others provide direct measurements of how much the signal is off, while a third group provides additional vehicle data for integration into the computation process.

A satellite-based augmentation system (SBAS) is a system that supports augmentation through the use of additional satellite-broadcast messages. Such systems are commonly composed of multiple ground stations, located at precisely-surveyed points. The ground stations take measurements of one or more of the GNSS satellites, the satellite signals, or other environmental factors, which may impact the signal received by the users. Using these observations, correction messages are created and sent to one or more satellites to be broadcast to the end users. SBAS is sometimes synonymous with WADGNSS, wide-area DGNSS. Examples of SBAS are the Wide Area Augmentation System (WAAS), operated by the United States Federal Aviation Administration (FAA) and the European Geostationary Navigation Overlay Service (EGNOS), operated by the European Satellite Services Provider (ESSP).

Ground-based augmentation systems (GBAS) and ground-based regional augmentation systems (GRAS) support augmentation through the use of messages transmitted by radio or mobile data networks. As with the satellite based augmentation systems detailed above, ground-based augmentation systems are commonly composed of one or more precisely-surveyed ground stations (references), which take measurements concerning the GNSS, and the data are transmitted directly to the end user (rover). The distance between the reference and the rover, *i.e.*, baseline, has a major influence on the achievable accuracy. Examples of GBAS utilizing DGNSS are real-time kinematic (RTK) measurements, where correction messages are typically received from one reference station, and the virtual reference station (VRS) service, where a network of reference stations is used to compute a virtual reference for a location close to the rover.

The augmentation can also include additional information being blended into the position computation. Often the additional positioning instruments used operate using principles that complement GNSS positioning. These instruments provide independent and uncorrelated data that are not necessarily subject to the same sources of error or interference. The additional sensors may include sensors such as an IMU, an electronic compass and an odometer.

2.3. Post-Processing of GNSS Data

If raw satellite observations of the reference and the rover are stored, the position of the rover can be computed in post-processing using DGNSS. Another method is to use only the data logged at the rover and precise point processing (PPP). The PPP approach utilizes precise clocks and orbits, two of the most significant error sources of GNSS positioning. GPS satellite ephemerides, satellite and ground station

clocks and GLONASS satellite ephemerides can be downloaded from International GNSS Service (IGS). These data are typically available after a couple of days (GPS) or two weeks (GLONASS) after the observation session [24]. Post-processing often results in better positioning accuracy, but, as a real-time method, it is highly dependent on the satellite visibility, instrumentation, *etc*. Data logged with additional sensors, such as an IMU and an odometer, can be used to improve the accuracy and reliability of the post-processed position solution.

2.4. GNSS in under Forest Canopies

There are many studies focusing on positioning under forest canopies using various GNSS devices and processing techniques, and the results show that a dense forest canopy can reduce the accuracy of the GNSS device. In these cases, the measurements were obtained during static sessions of varying length, and the positioning accuracy varied from a few centimeters to several meters, depending on the instrumentation, length of data observation period, and processing.

Næsset and Gjevestad [25] studied the performance of a GPS PPP application under coniferous forest canopies. A 20-channel, dual-frequency GPS receiver collecting pseudorange and carrier phase observations was used as a stand-alone receiver to determine the positional accuracy of 19 points under coniferous forest canopies. The mean positional accuracy ranged from 0.27 to 0.88 m for an observation period of 120 min, and 0.95 to 3.48 m for 15 min. In the case of the 15 min observation period, the computed positions could not be found for 8 to 44 percent of the locations. The accuracy increased as the forest stand density decreased. The stand basal area and number of trees correlated significantly with the expected positioning accuracy.

The accuracies of recreational-grade and survey-grade GPS receivers were evaluated by Andersen *et al.* [26] across a range of forest conditions in the Tanana Valley of interior Alaska. High-accuracy check points were then used to evaluate the accuracy of positions acquired in stands representing different forest types using a recreational-grade GPS unit and a GLONASS-enabled survey-grade unit, over a range of acquisition and post-processing alternatives, including distance to base station, or baseline length (0–10, 10–50, 50–100, and >100 km), use of GLONASS satellites, and data observation periods (5, 10, and 20 min). The accuracy of the recreational-grade GPS was 3–7 m across all sites. As regards the survey-grade units, their accuracy was influenced by the forest type and baseline length, with smaller errors observed in more open stands and with shorter baseline lengths. The use of GLONASS satellites improved positioning accuracy by a small but appreciable amount, and longer observation periods (20 min) resulted in more reliable and accurate positions across all sites. In general, these results indicate that if forest inventory plots in interior Alaska and other high-latitude regions of the world were occupied for 20 min by survey-grade instruments, positioning accuracy below 1 m errors can be consistently obtained across a wide range of conditions.

Danskin *et al.* [27] confirmed that survey-grade receivers provide higher horizontal positioning accuracy than consumer-grade receivers, better horizontal positioning accuracy during leaf-off forest conditions (*i.e.*, winter), and that differential correction can improve horizontal positioning accuracy, and WAAS, when available, can improve horizontal positioning accuracy.

Even centimeter-level accuracy can be achieved using differential computation and static observations, but usually this requires open-sky conditions [28,29].

However, positioning while moving is a more complex problem as satellite visibility changes arbitrarily and the collecting of positional reference data is challenging. There are some studies addressing the positioning accuracy of a moving device evaluated under a forest canopy. Tachiki *et al.* [30] studied GPS-related positional errors produced when monitoring a mobile device under the forest canopy on two test sites: a deciduous forest stand and a coniferous forest stand with mean stand tree heights 8.4 and 8.9 m, and mean basal areas 41.1 and 38.4 m^3/ha, respectively. Two GPS receivers were used, one of navigation-grade and the other of survey-grade, both with and without real-time differential correction. The mean horizontal accuracy (STD) was about 4.1 m for the navigation-grade receiver and about 2.7 m for the survey-grade receiver. Differential correction did not improve the accuracy for either receiver. The researchers concluded that a higher stand density causes a larger positional error when the basal area is about the same. Ucar *et al.* [31] studied the dynamic accuracy of recreational-grade GPS receivers in an oak-hickory forest by measuring the area of the test plot (0.9 ha) defined by eight ground-based control points. They concluded that the average area agreement was 93% during the winter season (leaf-off), and 84% during the summer season (leaf-on). In the study by Liang *et al.* [32], the accuracy of estimation of the location of the tree stems when using a mobile laser scanning system setup in a backpack was 0.38 m. The main error source was in the positioning of the system. The study area was a homogenous mature pine forest and an IMU was used and post-processing was implemented.

Past studies have concentrated on the positioning accuracy of GNSS in forest environments and on techniques for improving GNSS accuracy. In 2001, Holden *et al.* [33] used skyward-looking photography in conjunction with GPS data in an attempt to develop a quantitative method of classifying forest canopies and of relating this classification to the degradation of carrier phase differential GPS (DGPS) performance. This technique led to a definite correlation between canopy obstruction and DGPS performance with the R^2 value increasing up to 0.74 when fitting a trend line to their findings. In 1999, Sigrist and Hermy [34] found that with 300 GPS fixes, the Position Dilution of Precision (PDOP) is not as good an indicator of positional accuracy under a forest canopy as has been generally acclaimed. The study focused on the quantitative analysis of GPS accuracy under different forest canopy types and how PDOP affects positional accuracy as well as how foliage relates to signal blockage. The most significant conclusions presented in this paper were as follows: as canopy density increased, the signal attenuation increased; PDOP is not a good indicator of position precision; and the usability of skyward photography techniques as a measure of canopy closure. Bettinger and Merry [35] also found moderate correlation between average positional error and some forest structure attributes in their study on the influence of the juxtaposition of trees on consumer-grade GPS positioning quality. In 1998, Axelrad and Behre [36] demonstrated that NMEA (National Marine Electronics Association) messages in GPS receivers included individual SV (space vehicle, satellite) signal to noise ratios and are capable of showing significant signal attenuation based on the angle of the SV from the zenith. This particular research was measuring this signal attenuation from space-based platforms and so the attenuation was mainly attributed to the atmosphere. It is, therefore, rational to assume that the addition of forest canopy between the SV and antenna attenuates the signal further. The technique of signal-to-noise ratios from each SV can provide us with the data from each SV and the SV location relative to the antenna regarding the effect of forest canopy density and the effect of the signal propagation of as caused by the forest.

3. Methods

3.1. General Workflow

Evaluation of the positioning accuracy of a moving vehicle under a forest canopy is quite a challenging task. To evaluate this, a test field consisting of four different forest stands was established. Several different combinations of GNSS and IMU were mounted on an all-terrain vehicle (ATV) (Figure 1). The positions of 224 trees along the driving route were measured using total-station and real-time kinematic GPS. These trees were used to form the network of reference objects. In addition to GNSS and IMU, a laser scanner was mounted on the ATV. Thus, when a laser point cloud was computed using the recorded GNSS and IMU observations and laser scanner measurements, the position of the ATV could be determined based on the reference objects, *i.e.*, trees, measured from the point cloud. The accuracy of the post-processed GNSS-IMU trajectory could be verified, and this trajectory was used as a reference for several other positioning systems. A large number of forest test plots 32 by 32 m in size were created along the trajectory, and the forest parameters for these test plots were estimated using up-to-date ALS data. This enabled the analysis of how forest parameters affect the accuracy of positioning.

Figure 1. An ATV with global satellite navigation systems (GNSS) antennas and receivers, inertial measurement unit (IMU) and laser scanner equipment mounted on it for the purposes of the study.

3.2. Test Field and Reference Data

Test field was established in the Evo study area located in southern Finland (61°19′ N, 25°11′ E). The area lies within the southern boreal forest zone and comprises approximately 2000 ha of mainly managed boreal forest. Scots pine and Norway spruce are the dominant tree species and the average stand size in the area is slightly less than one hectare. The elevation of the area varies from 125 to 185 m above sea level.

In the first phase, an ATV route 800 m in length was laid out to cross four forest stands. Then 224 trees were marked on either side of the route (Figure 2). The locations of the trees were measured to the center of the stem at breast height (1.3 m above ground level) using a Trimble 5602 DR200+ total station. The total-station orientations were determined using ground-control points measured in open areas around

the test site using a VRS-GPS device. The measured trees comprised the reference object network. The location accuracy of the reference targets was estimated to be better than 10 cm in 2D (East–North). The route was driven two times to acquire data with different satellite geometry (Table 1). The average driving speed of the ATV was about 4 km/h.

Figure 2. The reference trajectory (red) and the reference trees (green). Background orthoimage: National Land Survey Finland 2012.

Table 1. Reference trajectory acquisition.

	Trajectory 1	***Trajectory 2***
Date	30 October 2014	30 October 2014
Start and end time (UTC+3)	12:01:32 p.m.–12:15:14 p.m.	2:26:04 p.m.–2:37:33 p.m.
No. of satellites, cut-off angle 15° [a]	13 (6 GPS + 7 GLO)	18 (10 GPS + 9 GLO)
GDOP, cut-off angle 15° [a]	2.8	1.9
Ionosphere Total Electron Content [a]	30 (low)	35 (low)
Average speed	3.5 km/h	4.2 km/h

[a]:Trimble Navigation Ltd., Sunnyvale, CA, USA, http://www.trimble.com.

The reference trajectory and laser scanning were collected using a MLS system ROAMER R2 of the Finnish Geospatial Research Institute, FGI. The ROAMER R2 consists of a NovAtel SPAN navigation system, which includes a GNSS receiver and an IMU, and an ultra-high speed phase-shift laser scanner. All sensors are mounted on a rigid platform. Tables 2 and 3 list the technical specifications of the navigation system and the laser scanner.

The reference trajectory was computed using the Waypoint Inertial Explorer software. The reference GNSS data were downloaded from the Trimnet GNSS service to a virtual reference station close to the test site. The collected laser point cloud was georeferenced to local coordinate system by combining the laser scanner data with the trajectory and synchronization data using FGI software developed in-house.

Table 2. The technical specifications of the navigation system (NovAtel SPAN GNSS-IMU [a]).

Unit	Features	Specifications
NovAtel Flexpak6 GNSS receiver and GPS-702-GG antenna	Frequencies	GPS L1 L2 L2C L5 GLONASS L1 L2
	Horizontal positioning accuracy (RMS) RTK	1 cm + 1 ppm
NovAtel UIMU-LCI Fiber optic gyro IMU	Output rate	200 Hz
	Acceleration accuracy (RMS)	0.004 m/s^2
	Gyro input range	±800 deg/s
	Gyro rate bias	<1.0 deg/h
	Gyro rate scale factor	100 ppm
	Angular random walk	<0.05 deg/√h
	Accelerometer range	±40 g
	Accelerometer bias	<1.0 mg

[a]: NovAtel Inc., Calgary, Canada, www.novatel.com.

Table 3. The technical specifications of the laser scanner (FARO Focus3D 120S [a]).

Features	Specifications
Maximum range	153 m
Vertical field of view	305°
Ranging error	±2 mm @ 25 m
Wavelength	905 nm
Beam divergence	0.19 mrad, 3 mm at exit
Scan frequency	3–97 Hz
Point repetition frequency	122–976 kHz
Angular resolution	0.02–5.0 mrad

[a]: FARO Focus3D Features, Benefits & Technical Specifications, Lake Mary, FL, USA, www.faro.com.

The reference positions of the trees were measured in the field at breast height, which was determined as 1.3 m above average ground level around the tree. Accordingly, the point cloud was classified for points on the ground and for points at 1.3 m above the ground. The ground-based points were classified using the ground classification algorithm in the TerraScan software (Terrasolid Ltd., Helsinki, Finland). This algorithm is based on the triangulated irregular network (TIN) approach using local low points as the initial points and then starts to grow a network of triangles according to the given parameters (for more details, see [37]). In this study, the parameters were optimized to produce a surface model that is sufficiently dense and follows also the smaller terrain variations, and yet excludes extreme noise. The parameters were: (1) Maximum building size: 1 m × 1 m. This is the maximum size of the local area where initial low points are searched for. (2) Terrain angle: 88°. This is the local maximum steepness of the surface model. (3) Iteration angle: 12°. This determines the maximum angle formed by the point, the closest triangle vertex, and the closest triangle plane. (4) Iteration distance: 1 m. This gives the maximum distance from a point to the nearest triangle plane.

The breast height level was then determined as the point within given height limits from the corresponding ground-based points. The height limits used were 1.2 and 1.4 m. These points on the tree stems were then visually identified. Their location and diameter at breast height (DBH) were measured

by fitting a circle around the stem points (Figure 3a): the location of the tree was thus the center coordinates of the circle and DBH was the diameter of the circle. The circles were fitted manually using visual interpretation. Finally, the median GPS time of the points found within each circle was calculated and matched with the location and diameter data.

The different driving directions were processed separately. In the case of "multiplied trees" near the turning points where trees had been scanned from several positions, each multiplication was measured individually (Figure 3b). The position error between the tree location in the point cloud and the corresponding reference tree location was then calculated for every tree and its multiplications were found in the point clouds. The median GPS time for each tree was used to study the variation in positioning error throughout the driving session.

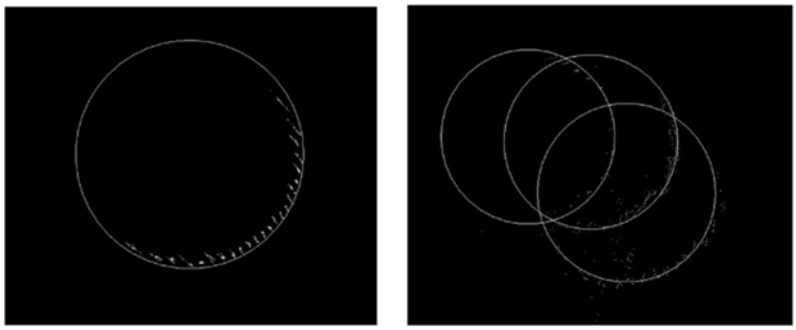

a **b**

Figure 3. Fitting a circle around the stem points of the MLS (Mobile Laser Scanning) reference (**a**) and same tree stem scanned from different locations with MLS showing the positioning error (**b**).

The accuracy of the reference trajectory was determined by comparing the tree locations derived from the total-station measurements with those measured from the point cloud. The RMSE values of the two reference trajectories are given in Table 4.

Table 4. The accuracy of the reference trajectories.

Trajectory	RMSE (m)		
	East	North	2D
Ref. trajectory 1	0.51	0.35	0.62
Ref. trajectory 2	0.45	0.64	0.79

3.3. The Tested GNSS Devices

The tested GNSS devices include a low-cost consumer handheld navigator, two single-frequency receivers with external mini-antennas, and a geodetic dual-frequency receiver with an external antenna (Table 5). All of these devices use GPS and GLONASS satellites for positioning, and they logged the positions in real-time during the two trajectory runs; the exception was NVS device, which encountered a logging problem during the second run. For comparison, a post-processed solution was also computed for the NVS and NovAtel receivers with Waypoint Inertial Explorer using default parameters for a

ground-based vehicle. The post-processing procedure was the same as for the computation of the reference trajectory (see Section 3.2.), but without using the IMU data.

Table 5. The tested GNSS devices.

Device	Type	Antenna
Garmin eTrex 30	Handheld single-frequency navigator	In-built
u-blox MAX-M5Q	Single-frequency receiver	External generic patch
NVS NV08C-CSM	Single-frequency receiver	Maxtena M1227HCT-A-SMA
NovAtel FlexPak6	Dual-frequency geodetic receiver	NovAtel GPS-702-GG

3.4. Stand Data Based on Forest Plots

Altogether 426 grid cells measuring 32 m by 32 m were created alongside the trajectory, with the center points of the cells following the trajectory. The forest inventory attributes for the grid cells were predicted using the ALS data (acquisition date 5 September 2014, point density 6 points per m^2), the field measurements of the sample plots with the respective size in the same area (n = 90), and an algorithm created at the FGI [38–40]. First, the point clouds from sample plot areas and grid cells were extracted from the ALS data and used to calculate the statistical parameters. The parameters were calculated from normalized ALS data above the threshold value of 2 m, *i.e.*, the points higher than 2 m above ground, and the parameters included minimum height, maximum height, mean height calculated as the arithmetic mean of laser-based heights, standard deviation of the heights, coefficient of variation, penetration, percentiles calculated from 10% to 90% of canopy height distribution at 10% intervals, and canopy cover percentiles expressed as the proportion of returns below a given percentage of total height from 10% to 90% of the heights. With all this done, the prediction model was developed based on these features and field-measured forest inventory attributes from 90 sample plots using random forest technique, which is a non-parametric regression technique. Finally, the forest inventory parameters for 426 grid cells were estimated based on the developed model and the ALS features derived for the areas. The predicted forest inventory parameters were mean tree height, mean DBH, basal area, volume, and biomass, in addition to the ALS penetration rate. The RMSE-% values achieved were 5.2% for mean tree height, 11.9% for mean DBH, 15.4% for basal area, 18.4% for volume, and 15.3% for biomass.

The stands were classified into four categories based on the mean tree height: young pine stand (<21 m), young spruce stand (21–25 m), mature pine stand (25–27.5 m), and mature spruce stand (>27.5 m). The general data on the stands is shown in Table 6.

Table 6. General data on the stands.

Stand Type	Mean Tree Height (m)	Mean DBH (cm)	Basal Area (m^2/ha)	Volume (m^3/ha)	Biomass (Mg/ha)	Penetration Rate (%)
Young pine	19.4	19.0	22.2	218.1	108.0	45.5
Young spruce	23.9	18.6	31.5	352.1	162.1	32.7
Mature pine	26.3	20.4	34.3	411.0	180.6	30.1
Mature spruce	28.7	22.2	37.3	447.4	197.1	26.0

3.5. Evaluation of Accuracy

The accuracy of different GNSS equipment positionings was evaluated by calculating the RMSE between the reference trajectory location (LOC_{REF}) and the GNSS location (LOC_{GNSS}) concurrently with GPS time at 1 sec intervals, Equation (1).

$$RMSE = \sqrt{\frac{\sum_{i=1}^{n}(LOC_{REFi} - LOC_{GNSSi})^2}{n}} \quad (1)$$

A single factor Analysis of Variance (ANOVA) was carried out to test whether the forest conditions had a significant effect on the results. The significance threshold was set at 0.05.

4. Results

The results for positioning accuracy under forest canopies are shown in Table 7. As regards NVS and NovAtel, both the real-time autonomous single-point solution and the post-processed differential solution are given. As can be seen, the real-time accuracy of single-frequency devices is superior to that of geodetic dual-frequency device equipped with a less sensitive antenna-receiver combination optimized for differential solution under better satellite visibility. High-sensitivity receivers are able to track weaker signals, which results in a larger number of tracked satellites, but the signals are subject to interference and multipathing due to disturbance caused by forest canopies. Geodetic receivers are also subject to interference and multipathing, but the tracked signals are of better quality in terms of frequency spectrum and measurement noise thanks to the purpose-designed antenna and signal-processing techniques. High-sensitivity receivers are mostly used in navigators and smartphones, and geodetic receivers have been adopted by professionals for geodetic purposes. When post-processing is applied, the accuracy of NovAtel improves notably and is superior to real-time solutions. With IMU data also available, the accuracy was 0.7 m (reference trajectory). During the data acquisition along Trajectory 2, there were five visible satellites more than were available for Trajectory 1, and this probably partly explains the better accuracy obtained with the real-time systems.

Table 7 The positioning accuracy under forest canopies.

Device (No. of Observations Traj.1/Traj.2)	RMSE (m)		Combined
	Traj.1	Traj.2	
Garmin eTrex 30 (823/690)	10.2	6.6	8.4
u-blox MAX-M5Q (823/690)	4.9	4.6	4.7
NVS single point (642/N/A)	6.2	N/A	N/A
NVS post-proc. GPS only (660/N/A)	6.7	N/A	N/A
NovAtel single point (768/654)	45.6	17.5	31.5
NovAtel post-proc. (556/400)	1.7	1.9	1.8

Traj.: trajectory.

On analyzing accuracy under different forest conditions, it appeared that the accuracy of single-frequency GNSS devices is less dependent on forest conditions, whereas the performance of the tested geodetic dual-frequency receiver is very sensitive to satellite visibility (Table 8). This can also be seen in the

post-processed solution for NovAtel; the accuracy deteriorated with increasing basal area, mean height, and stem volume.

Table 8. The positioning accuracy under different forest stand conditions and the resultant ANOVA values.

Device	RMSE (m), Mean of Two Runs (No. of Observations)				ANOVA	
	Young Pine	Young Spruce	Mature Pine	Mature Spruce	F	*p*-Value
Garmin eTrex 30	9.3 (277)	8.5 (249)	8.2 (709)	7.7 (278)	20.0	<0.001
u-blox MAX-M5Q	4.2 (277)	4.8 (249)	4.7 (709)	4.6 (278)	10.0	<0.001
NVS single point	5.5 (123)	6.8 (76)	6.1 (336)	6.8 (118)	3.00	0.030
NVS post-proc. GPS only	5.9 (124)	7.7 (84)	6.6 (338)	6.9 (114)	2.85	0.036
NovAtel single point	7.6 (272)	31.4 (229)	27.2 (672)	49.3 (249)	4.01	0.007
NovAtel post-proc.	0.8 (249)	1.3 (145)	1.9 (524)	2.7 (123)	71.63	<0.001

5. Discussion and Conclusions

The aim of this study was to investigate the positioning accuracy of novel GNSS devices under forest canopies representing varying forest conditions. The study was carried out to simulate the accuracy that could be obtained when using a harvester. The acquisition of detailed and spatially accurate tree data is required in forest inventories based on remote sensing for ground-based truth, and a harvester in motion is one potential data source for such data [4,9,15,39,40].

Based on the results, the required accuracy level of 1 m for tree matching cannot be achieved when using stand-alone GNSS devices, but when differential GNSS (real-time or post-processed) together with IMU data are applied, accuracy of even less than 1 m can be achieved, e.g., in this study this was 0.6–0.8 m. Thus, in theory, if high-precision GNSS + IMU units are mounted onto a harvester, then the collected stem data can be linked to remote-sensing data and further utilized in forest-inventory applications. However, the fusion of harvester data and remote-sensing data warrants further research. The present study addressed only the positional problem studied using an ATV instead of a harvester. In practice, unlike the ATV in this study, the harvester is not constantly on the move, and the satellite antenna is located higher above the ground [41], and consequently improved accuracy in real-life scenario can be expected under similar forest conditions. On the other hand, satellite geometry is continually changing, and (even though the test data were collected at different times of the day) positioning accuracy may improve or deteriorate from what is reported here as "satellite conditions" change. The remote sensing part of the method has been studied by Holmgren *et al.* [16], who looked into the prediction of basic stand variables, such as stem volume, mean tree height, diameter, and stem density, and used manually taken measurements to match the logged trees with the ALS data since the harvesters cannot provide the needed positioning.

The RMSE of real-time 2D GNSS positioning for single-frequency receivers varied between 4 and 9 m in mature and thinning stands. This level of accuracy is not adequate to enable the accurate determination of the real-time position of a moving vehicle within the forest. However, the accuracy improves when the harvester remains stationary for longer periods. It seems that the accuracy of novel single-frequency GNSS devices is not so dependent on the forest conditions, whereas the performance of the tested geodetic dual-frequency receiver appears to be more sensitive to satellite visibility. In situations where

post-processing and dual-frequency satellite data can be applied, accuracy of up to 2 m can be obtained for a slowly moving vehicle.

Acknowledgments

This study was made possible by financial aid from the Finnish Academy projects "Towards Precision Forestry", "Centre of Excellence in Laser Scanning Research (CoE-LaSR) (272195)", "Interaction of Lidar/Radar Beams with Forests Using Mini-UAV and Mobile Forest Tomography", "Competence Based Growth Through Integrated Disruptive Technologies of 3D Digitalization, Robotics, Geospatial Information and Image Processing/Computing Point Cloud Ecosystem" and from DIGILE's Data to Intelligence Program. The research leading to these results has received funding from the European Community's Seventh Framework Programme ([FP7/2007–2013]) under grant agreement No. 606971. The authors wish to thank Ponsse PLC for providing a GNSS device for the test.

Author Contributions

Harri Kaartinen is the main author of the article, analyzing and reporting the achieved results. Juha Hyyppä and Mikko Vastaranta have contributed especially in regard to the forestry-related matters. Harri Kaartinen, Mikko Vastaranta, Antero Kukko, Anttoni Jaakkola, Xinlian Liang, Jingbing Liu, Risto Kaijaluoto, and Timo Melkas designed and executed the field data collection. Xiaowei Yu processed the ALS data and predicted the forest inventory parameters. Harri Kaartinen, Antero Kukko, and Jiri Pyörälä processed the reference data. The article was improved by the contributions of all the co-authors at various stages of the analysis and writing.

Conflicts of Interest

The authors declare no conflict of interest.

References

1. Næsset, E.; Gobakken, T.; Holmgren, J.; Hyyppä, H.; Hyyppä, J.; Maltamo, M.; Nilsson, M.; Olsson, H.; Persson, Å.; Söderman, U. Laser scanning of forest resources: The Nordic experience. *Scand. J. For. Res.* **2004**, *19*, 482–499.
2. McRoberts, R.E.; Tomppo, E.O.; Næsset, E. Advances and emerging issues in national forest inventories. *Scand. J. For. Res.* **2010**, *25*, 368–381.
3. Wulder, M.A.; White, J.C.; Nelson, R.F.; Næsset, E.; Ørka, H.O.; Coops, N.C.; Hilker, T.; Bater, C.W.; Gobakken, T. Lidar sampling for large-area forest characterization: A review. *Remote Sens. Environ.* **2012**, *121*, 196–209.
4. Hyyppä, J.; Inkinen, M. Detecting and estimating attributes for single trees using laser scanner. *Photogramm. J. Finl.* **1999**, *16*, 27–42.
5. Persson, A.; Holmgren, J.; Söderman, U. Detecting and measuring individual trees using an airborne laser scanner. *Photogramm. Eng. Remote Sens.* **2002**, *68*, 925–932.
6. Peuhkurinen, J.; Maltamo, M.; Malinen, J.; Pitkänen, J.; Packalén, P. Preharvest measurement of marked stands using airborne laser scanning. *For. Sci.* **2007**, *53*, 653–661.

7. Villikka, M.; Maltamo, M.; Packalén, P.; Vehmas, M.; Hyyppä, J. Alternatives for predicting tree-level stem volume of Norway spruce using airborne laser scanner data. *Photogramm. J. Finl.* **2007**, *20*, 33–42.
8. Vauhkonen, J.; Tokola, T.; Packalén, P.; Maltamo, M. Identification of Scandinavian commercial species of individual trees from airborne laser scanning data using alpha shape metrics. *For. Sci.* **2009**, *55*, 37–47.
9. Yu, X.; Hyyppä, J.; Vastaranta, M.; Holopainen, M.; Viitala, R. Predicting individual tree attributes from airborne laser point clouds based on the random forests technique. *ISPRS J. Photogramm. Remote Sens.* **2011**, *66*, 28–37.
10. Melkas, T. Wood Measuring Methods Used in Finland 2013. Available online: http://www.metsateho.fi/wp-content/uploads/2015/02/Tuloskalvosarja_2014_09b_Wood_measuring_methods_used_in_Finland_2013_tm.pdf (accessed on 2 June 2015).
11. StanForD. Standard for Forest Machine Data and Communication. Available online: http://www.skogforsk.se/english/projects/stanford/ (accessed on 2 June 2015**)**.
12. Rasinmäki, J.; Melkas, T. A method for estimating tree composition and volume using harvester data. *Scand. J. For. Res.* **2005**, *20*, 85–95.
13. Holopainen, M.; Hyyppä, J.; Vaario, L.; Yrjälä, K.; Mery, G.; Katila, P.; Galloway, G.; Alfaro, R.; Kanninen, M.; Lobovikov, M. Implications of technological development to forestry. *For. Soc. Responding Global Driv. Chang.* **2010**, *25*, 157–182.
14. Vastaranta, M.; Holopainen, M.; Yu, X.; Hyyppä, J.; Mäkinen, A.; Rasinmäki, J.; Melkas, T.; Kaartinen, H.; Hyyppä, H. Effects of individual tree detection error sources on forest management planning calculations. *Remote Sens.* **2011**, *3*, 1614–1626.
15. Kaartinen, H.; Hyyppä, J.; Yu, X.; Vastaranta, M.; Hyyppä, H.; Kukko, A.; Holopainen, M.; Heipke, C.; Hirschmugl, M.; Morsdorf, F. An international comparison of individual tree detection and extraction using airborne laser scanning. *Remote Sens.* **2012**, *4*, 950–974.
16. Holmgren, J.; Barth, A.; Larsson, H.; Olsson, H. Prediction of stem attributes by combining airborne laser scanning and measurements from harvesters. *Silva Fenn.* **2012**, *46*, 227–239.
17. Melkas, T.; Vastaranta, M.; Haapanen, R.; Holopainen, M.; Yu, X.; Hyyppä, J.; Hyyppä, H. Updating forest resource data by using ALS measurements and information collected with a harvester. In Proceedings of SILVILASER 2009: The 9th international conference on lidar applications for assessing forest ecosystems, College Station, TX, USA, 14–16 October 2009; pp. 128–136.
18. Næsset, E. Predicting forest stand characteristics with airborne scanning laser using a practical two-stage procedure and field data. *Remote Sens. Environ.* **2002**, *80*, 88–99.
19. Bettinger, P.; Tang, M. Tree-Level Harvest Optimization for Structure-Based Forest Management Based on the Species Mingling Index. *Forests* **2015**, *6*, 1121–1144.
20. Finnish Geospatial Research Institute FGI. Satellite-Based Positioning Systems. Available online: http://www.fgi.fi/fgi/themes/satellite-based-positioning-systems (accessed on 24 March 2015).
21. Official U.S. Government information about the Global Positioning System (GPS) and related topics. Space Segment. Available online: http://www.gps.gov/systems/gps/space/ (accessed on 24 March 2015).
22. Poutanen, M. *GPS-Paikanmääritys*; Tähtitieteellinen yhdistys Ursa: Helsinki, Finland, 1998.

23. European Space Agency (ESA). What is Galileo?/The Future—Galileo/Navigation/Our Activities. Available online: http://www.esa.int/Our_Activities/Navigation/The_future_-_Galileo/What_is_Galileo (accessed on 24 March 2015).
24. International GNSS Service. IGS Products. Available online: http://igs.org/products (accessed on 24 March 2015).
25. Næsset, E.; Gjevestad, J.G. Performance of GPS precise point positioning under conifer forest canopies. *Photogramm. Eng. Remote Sens.* **2008**, *74*, 661–668.
26. Andersen, H.-E.; Clarkin, T.; Winterberger, K.; Strunk, J. An accuracy assessment of positions obtained using survey-and recreational-grade global positioning system receivers across a range of forest conditions within the Tanana valley of interior Alaska. *Western J. Appl. For.* **2009**, *24*, 128–136.
27. Danskin, S.D.; Bettinger, P.; Jordan, T.R.; Cieszewski, C. A comparison of GPS performance in a southern hardwood forest: Exploring low-cost solutions for forestry applications. *South. J. Appl. For.* **2009**, *33*, 9–16.
28. Bakuła, M.; Oszczak, S.; Pelc-Mieczkowska, R. Performance of RTK positioning in forest conditions: Case study. *J. Surv. Eng.* **2009**, *135*, 125–130.
29. Bakula, M.; Przestrzelski, P.; Kazmierczak, R. Reliable technology of centimeter GPS/GLONASS surveying in forest environments. *IEEE Trans. Geosci. Remote Sens.* **2015**, *53*, 1029–1038.
30. Tachiki, Y.; Yoshimura, T.; Hasegawa, H.; Mita, T.; Sakai, T.; Nakamura, F. Effects of polyline simplification of dynamic GPS data under forest canopy on area and perimeter estimations. *J. For. Res.* **2005**, *10*, 419–427.
31. Ucar, Z.; Bettinger, P.; Weaver, S.; Merry, K.L.; Faw;K. Dynamic accuracy of recreation-grade GPS receivers in oak-hickory forests. *Forestry* **2014**, *87*, 504–511.
32. Liang, X.; Kukko, A.; Kaartinen, H.; Hyyppä, J.; Yu, X.; Jaakkola, A.; Wang, Y. Possibilities of a personal laser scanning system for forest mapping and ecosystem services. *Sensors* **2014**, *14*, 1228–1248.
33. Holden, N.; Martin, A.; Owende, P.; Ward, S. A method for relating GPS performance to forest canopy. *Int. J. For. Eng.* **2001**, *12*, 51–56.
34. Sigrist, P.; Coppin, P.; Hermy, M. Impact of forest canopy on quality and accuracy of GPS measurements. *Int. J. Remote Sens.* **1999**, *20*, 3595–3610.
35. Bettinger, P.; Merry, K.L. Influence of the juxtaposition of trees on consumer-grade GPS position quality. *Math. Comput. For. Nat. Resour. Sci.* **2012**, *4*, 81–91.
36. Axelrad, P.; Behre, C.P. Satellite attitude determination based on GPS signal-to-noise ratio. *Proc. IEEE* **1999**, *87*, 133–144.
37. Axelsson, P. Dem generation from laser scanner data using adaptive TIN models. *Int. Arch. Photogramm. Remote Sens.* **2000**, *33*, 111–118.
38. Breiman, L. Random forests. *Mach. Learn.* **2001**, *45*, 5–32.
39. Hyyppä, J.; Hyyppä, H.; Leckie, D.; Gougeon, F.; Yu, X.; Maltamo, M. Review of methods of small-footprint airborne laser scanning for extracting forest inventory data in boreal forests. *Int. J. Remote Sens.* **2008**, *29*, 1339–1366.
40. Yu, X.; Hyyppä, J.; Holopainen, M.; Vastaranta, M. Comparison of area-based and individual tree-based methods for predicting plot-level forest attributes. *Remote Sens.* **2010**, *2*, 1481–1495.

41. Brach, M.; Zasada,M. The effect of mounting height on GNSS receiver positioning accuracy in forest conditions. *Croat. J. For. Eng.* **2014**, *35*, 245–253.